

Full Paper

3D Pharmacophore Models for 1,2,3,4-Tetrahydroisoquinoline Derivatives Acting as Anticonvulsant Agents

Laura De Luca¹, Rosaria Gitto¹, Maria Letizia Barreca¹, Roberta Caruso¹, Silvana Quartarone¹, Rita Citraro², Giovambattista De Sarro², Alba Chimirri¹

¹ Dipartimento Farmaco-Chimico, Università di Messina, Messina, Italy

² Dipartimento di Medicina Sperimentale e Clinica, Università Magna Græcia, Catanzaro, Italy

A 3D pharmacophore model predicting anticonvulsant activity was obtained for a series of 6,7-dimethoxy-1,2,3,4-tetrahydroisoquinoline derivatives recently disclosed as a new class of non-competitive AMPA receptor antagonists. The training set included 17 compounds with varying potency against audiogenic seizures in DBA/2 mice. The best statistical hypothesis, generated with the HypoGen module of Catalyst 4.9, consisted of five features: two hydrogen bond acceptors, two hydrophobic features, and one hydrophobic aromatic region, providing a model with a correlation coefficient of 0.919. The obtained model was an efficient tool in the design of some new anticonvulsant agents containing the tetrahydroisoquinoline scaffold. Moreover, in order to explain the different degree of efficacy of the newly designed *N*-substituted derivatives, excluded volumes were also considered.

Keywords: AMPA receptor / Anticonvulsant agents / HypoGen / Isoquinolines / Pharmacophore model

Received: February 6, 2006; accepted: March 16, 2006

DOI 10.1002/ardp.200600022

Introduction

Glutamate (Glu), the major excitatory neurotransmitter in the vertebrate brain, plays an important role in neuronal activity operating through ionotropic (iGluRs) and metabotropic (mGluRs) receptors. The iGluRs are involved in many different physiological processes such as neuronal development, learning, and memory. However, their excessive activation is held responsible for the destruction of neuronal cells during several neurological diseases [1]. iGluRs are divided into *N*-methyl-D-aspartic acid (NMDA), 2-amino-3-(3-hydroxy-5-methylisoxazol-4-yl)propionic acid (AMPA), and kainate (KA) receptors, based on their pharmacology and structural properties. It is well known that competitive and noncompetitive antagonists of AMPA receptor (AMPA) show to be promising in terms of their therapeutic potential for the prevention and treatment of a broad range of acute and

chronic disorders [2, 3]. In particular, some 2,3-benzodiazepines (**1–3**, Fig. 1) [4, 5] were identified as marked anti-epileptic agents in various seizure models interacting with AMPA receptor complex in a selective and noncompetitive fashion. Among them, talampanel **1** has shown positive results in patients with severe epilepsy not responsive to other drugs and phase III trials are under way to confirm these results [6].

AMPA receptors are constituted as a heteromeric assembly of the subunits GluR1-4 which, in different combinations, produce receptors with distinct properties. The AMPA competitive agonist/antagonist binding site is located within the extracellular region of membrane protein. In particular, the application of X-ray diffraction has elucidated the structure of GluR2 bound with a series of competitive agonists/antagonists, providing some details about the ligand recognition and the activation-deactivation mechanism [7, 8]. On the contrary, no X-ray structure of any complex between noncompetitive antagonists and their binding site has been reported as yet and little information is available about the mechanism and impact of positive and negative modulator interaction [9]. Due to this lack of structural information and

Correspondence: Laura De Luca and Rosaria Gitto, University of Messina, Medicinal Chemistry, Viale Annunziata, Messina 98168, Italy.

E-mail: ldeluca@pharma.unime.it, gittoros@pharma.unime.it

Fax: +39 90 355-613

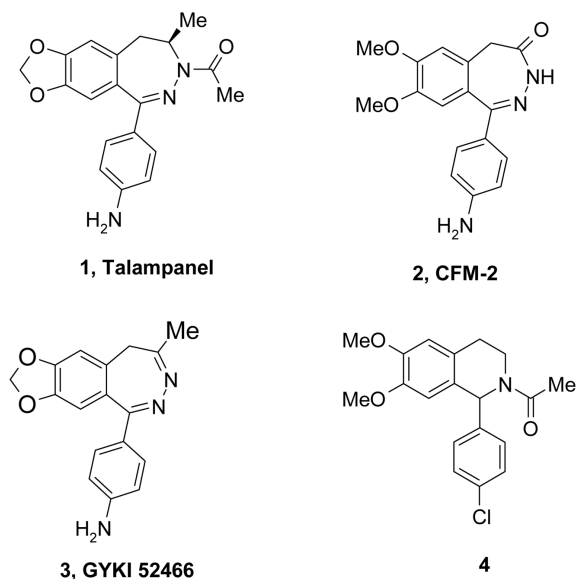


Figure 1. Negative allosteric modulator of the AMPA receptor.

ongoing with our research in this field [10], we have recently reported a hypothetical 3D ligand-based pharmacophore model by using the hypothesis generation approach HipHop/Catalyst [11].

The aim of this study was to identify the 3D structural requirements that are relevant in a molecule in order to noncompetitively interact with AMPAR and to produce anticonvulsant activity. The obtained common-features hypothesis, consisting of two hydrophobic regions, one hydrogen bond acceptor (HBA) and one aromatic region, was successfully used as a framework for the design of a new class of noncompetitive AMPAR antagonists and led to the discovery of 6,7-dimethoxy-1,2,3,4-tetrahydroisoquinoline derivatives as new potent anticonvulsant agents [11]. In particular, the 2-acetyl-1-(4-chlorophenyl)-6,7-dimethoxy-1,2,3,4-tetrahydroisoquinoline (**4**, Fig. 1) was characterized by improved pharmacological effects when compared in *in vivo* and *in vitro* tests with other current AMPAR antagonists **1–3** [12].

In this paper, we describe the automated generation of reliable 3D predictive pharmacophore models for 1,2,3,4-tetrahydroisoquinoline derivatives, in order to gain more insight into the structure activity-relationships (SAR) for this class of anticonvulsant drugs.

Results and discussion

Pharmacophore modeling

We used the algorithm HypoGen implemented in the Catalyst molecular modeling software [13] with the efforts to quantitatively correlate the chemical struc-

tures of a series of 1,2,3,4-tetrahydroisoquinoline derivatives, previously designed and synthesized by us [12, 14, 15], to their biological activity. The input for HypoGen run was a training set (TS) of 17 compounds **4–20** (Table 1).

Table 1 reports the molecules of our TS with the corresponding anticonvulsant activity value against audiogenic seizures in DBA/2 mice, which has been considered an excellent animal model for generalized epilepsy and for screening new anticonvulsant agents.

For our SAR study, we chose to use only the ED₅₀ values in the clonic phase of seizures, since the activities versus the clonic and tonic phases were highly correlated ($r^2 = 0.901$).

All molecular structures were sketched within Catalyst and minimized to their closest local energy minimum using a molecular mechanics approach. Poled conformations were generated for each molecule using the “best” conformer generation option and an energy cutoff of 10 kcal/mol.

Upon inspection of the structures and on the basis of our previous studies, it was determined that four generic types of chemical features described most of the functionalities of TS molecules. Therefore, HypoGen was instructed to select pharmacophore models using a hydrogen bond acceptor (HBA), hydrogen bond donor (HBD), hydrophobic (HY), hydrophobic aromatic (HYAr), and positive ionizable (P) groups.

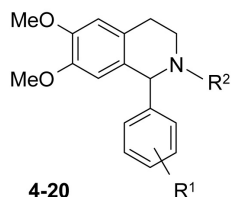
During the hypothesis generation process, Catalyst selects the best hypotheses of many possibilities by applying a cost analysis.

A set of ten hypotheses was thus generated using the data from TS compounds having correlation coefficients ranging from 0.772 to 0.919.

In order to evaluate if the obtained correlations were true and not due to chance, we have investigated the three cost values calculated by HypoGen and crucial in the validation of a reported hypothesis: the fixed cost, the null cost, and the total cost (section 4, Experimental).

In this study, the fixed cost of 45.6 bits was well separated from the null cost of 120.3 bits, and the difference between these two values of 74.7 bits underscored a high probability of generating useful models. Moreover, Catalyst documentation suggested that the goal of hypothesis generation is to obtain a set of hypotheses with total costs as close as possible to the fixed cost; our ten pharmacophore models fully satisfied this requirement as the total costs of the ten top-scored hypotheses range from 66.101 to 86.270.

The above-reported theoretical parameters thus revealed statistical significance of the optimized models generated with the HypoGen algorithm.

Table 1. Anticonvulsant activity of tetrahydroisoquinolines 4–20 against audiogenic seizures in DBA/2 mice.

Compd.	R ¹	R ²	ED ₅₀ μmol/kg ^{a)} (± 95% confidence limits)	
			clonic phase	tonic phase
4 ^{b)}	4 - Cl		4.18 (2.23 - 7.84)	2.39 (1.30 - 4.40)
5 ^{c)}	4 - Br		12.7 (6.09 - 26.3)	8.17 (4.03 - 16.6)
6 ^{d)}	3 - NO ₂	H	19.3 (6.10 - 61.2)	7.20 (2.45 - 21.2)
7 ^{d)}	4 - Cl	H	20.1 (9.65 - 41.9)	19.3 (11.8 - 31.5)
8 ^{c)}	4 - Cl		24.7 (13.2 - 46.2)	11.8 (8.10 - 17.0)
9 ^{d)}	3 - NH ₂		29.9 (17.5 - 50.9)	17.6 (10.4 - 29.7)
10 ^{b)}	4 - NH ₂		32.1 (17.7 - 58.3)	21.1 (11.0 - 40.4)
11 ^{b)}	4 - F		36.8 (20.6 - 65.8)	18.0 (7.76 - 41.8)
12 ^{d)}	H	H	44.8 (23.9 - 84.0)	19.3 (9.05 - 41.3)
13 ^{c)}	H		49.1 (36.9 - 65.5)	34.8 (19.6 - 61.6)
14 ^{b)}	H		53.5 (37.6 - 76.2)	37.7 (21.2 - 67.0)
15 ^{d)}	2,3 - Cl ₂		63.3 (35.8 - 111)	32.8 (17.5 - 61.5)
16 ^{c)}	4 - F		71.7 (64.6 - 110)	46.9 (21.3 - 103)
17 ^{c)}	4 - F		82.8 (54.1 - 126)	63.0 (32.8 - 101)
18 ^{d)}	3 - F	H	96.9 (60.5 - 155)	53.5 (38.3 - 73.8)
19 ^{d)}	4 - NO ₂	H	100 (52.1 - 194)	56.1 (26.9 - 117)
20 ^{d)}	2,3 - F ₂	H	130 (74.0 - 233)	48.1 (25.4 - 91.2)

a) All data were calculated according to the method of Litchfield and Wilcoxon [23]. At least 32 animals were used to calculate each ED₅₀.

b) Reference [12].

c) Reference [15].

d) Reference [14].

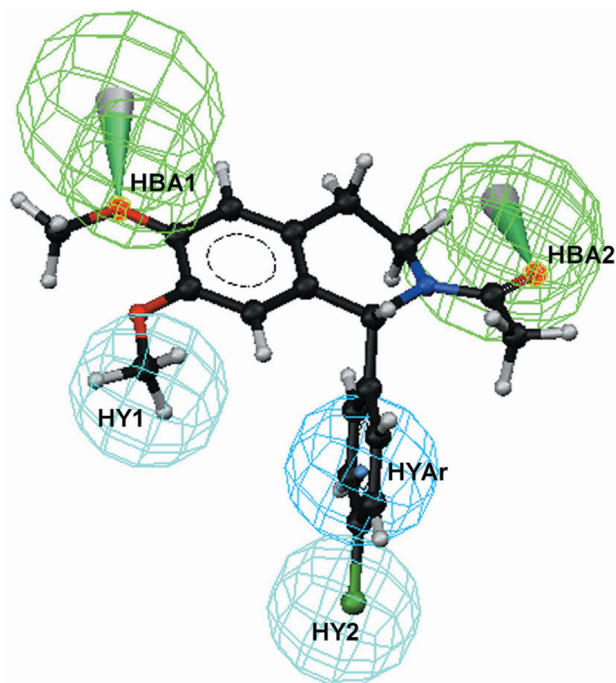


Figure 2. Best HypoGen pharmacophore model Hypo1 aligned to compound **4**. The pharmacophore features are color-coded as follows: green, hydrogen bond acceptor (HBA1 and HBA2); blue, hydrophobic aromatic region (HYAr,); cyan, hydrophobic group (HY1 and HY2).

The first output hypothesis (Hypo1) showed the best correlation coefficient (0.92), the lowest root-mean-square divergence (1.27), and a good cost difference (54.23) and it was chosen for further analysis.

Hypo1 consisted of five features: two HBAs, one HYAr, and two HYs located at defined positions.

Figure 2 shows Hypo1 aligned to the most active compound **4**, obtained by using the BestFit compare option of the View Hypothesis Workbench.

Compound **4** mapped well onto the five chemical functionalities of the 3D pharmacophore model: particularly, the two hydrogen bond regions were occupied by the carbonyl oxygen of the acetyl moiety and the oxygen atom of methoxy group at C-6, the aryl group filled the aromatic hydrophobic feature, whereas the 7-methoxy group and 4'-substituent overlapped with the two hydrophobic sites.

This model also accurately estimated the ED_{50} value of this molecule (predicted ED_{50} of 4.18 $\mu\text{mol/kg}$ vs. an experimental value of 4.80 $\mu\text{mol/kg}$). Moreover, comparison between the estimated activities and experimentally measured values for all compounds in the TS showed that the error costs (expressed as the ratio between the estimated and the experimental activities or its negative inverse if the ratio is less than one) were always < 10, indi-

Table 2. Experimental and estimated ED_{50} ($\mu\text{mol/kg}$) of TS molecules based on the pharmacophore model Hypo1.

Compd.	Experimental ED_{50} ($\mu\text{mol/kg}$)	Estimated ED_{50} ($\mu\text{mol/kg}$)	Error cost ^{a)}
4	4.2	4.8	+1.1
5	13	23	+1.8
6	19	20	+1
7	20	18	-1.1
8	25	19	-1.3
9	30	36	+1.2
10	32	34	+1.1
11	37	38	+1
12	45	96	+2.1
13	49	36	-1.4
14	53	34	-1.6
15	63	50	-1.3
16	72	74	+1
17	83	50	-1.7
18	97	98	+1
19	100	140	+1.4
20	130	97	-1.3

^{a)} The error cost values for all TS compounds, expressed as the ratio between the estimated and experimental activities or its negative inverse if the ratio is less than one, were found to be < 10, implying not more than one order difference between estimated and actual activity.

cating a reliable ability to estimate the biological activity (Table 2).

It is worth noting that Hypo1 describes some chemical features which were highlighted in our previous publication [11], confirming that the presence of the hydrogen-bond acceptor (HBA2), such as an acetyl moiety, and the aryl substituent (HYAr) are important for the binding interaction with the AMPA receptor complex. In addition, this hypothesis gave new information about the influence of other substituents on the pharmacological profile of tetrahydroisoquinoline derivatives.

On the basis of these results and in order to approve the predictive power of the quantitative model, we designed new potential AMPAR ligands (Fig. 3). Using the resulting five chemical feature hypothesis and the most active compound **4** as template, we planned from time to time the synthesis of different series of isoquinolines **21**, **22**, **23**, **24**, **25**, **26**, and **27** bearing modifications in three different positions of tetrahydroisoquinoline skeleton (see Fig. 3). Furthermore, in order to identify the contribution of the substitution pattern on the C-1 phenyl ring, we also synthesized derivatives **a–f** for each series.

At first, we have performed the computational design of derivatives **21a–f** (Fig. 3), in which the 1-aryl-6,7-dimethoxyisoquinoline scaffold was maintained, whereas the acetyl moiety was removed and a carbonyl group inserted on the isoquinoline skeleton. In fact, con-

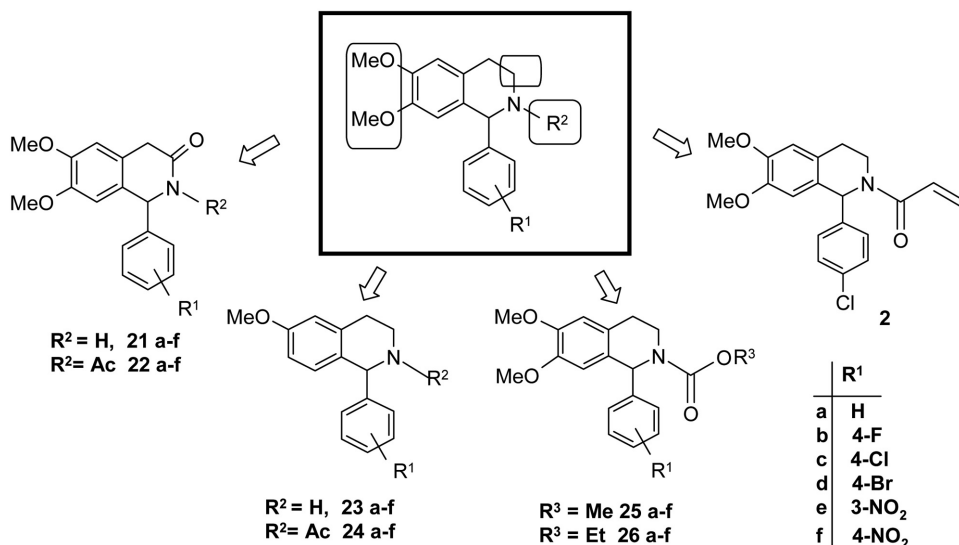
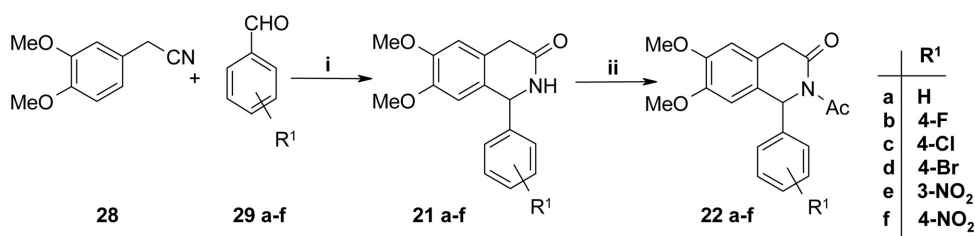


Figure 3. Planned structural modifications.



Scheme 1. Synthesis route for 1-aryl-6,7-dimethoxy-1,2-dihydroisoquinolin-3(4H)-ones **21a–f** and **22a–f**.

sidering that the presence of a chemical feature able to engage H-bond interaction (*i.e.* HBA2) appeared essential for anticonvulsant activity, we thought that the acetyl moiety could be suitably replaced by another hydrogen bond acceptor group with the same spatial location. So, 1-aryl-6,7-dimethoxy-1,2-dihydroisoquinolin-3(4H)-ones **21a–f** were synthesized, see section 2.2 (Chemistry) and Scheme 1, and tested against audiogenic seizures in DBA/2 mice (Table 3). In this class, compound **21c**, which mapped well onto Hypo1 (Fig. 4), was an efficacious anticonvulsant agent with ED₅₀ value of 23.4 $\mu\text{mol/kg}$ for the clonic phase of the test comparable to that of talampanel **1** (ED₅₀ = 13.4 $\mu\text{mol/kg}$) and higher than GYKI 52466 **3** (ED₅₀ = 35.8 $\mu\text{mol/kg}$). Biological data for **21c** was in perfect agreement with the *in silico* activity (20.0 $\mu\text{mol/kg}$).

We have also synthesized the 3-acetyl derivatives **22a–f** which proved to be less active than the corresponding N-unsubstituted analogues **21a–f** (Table 3), thus suggesting that the contemporaneous introduction of the acetyl moiety and the carbonyl function in these compounds is detrimental for the anticonvulsant potency.

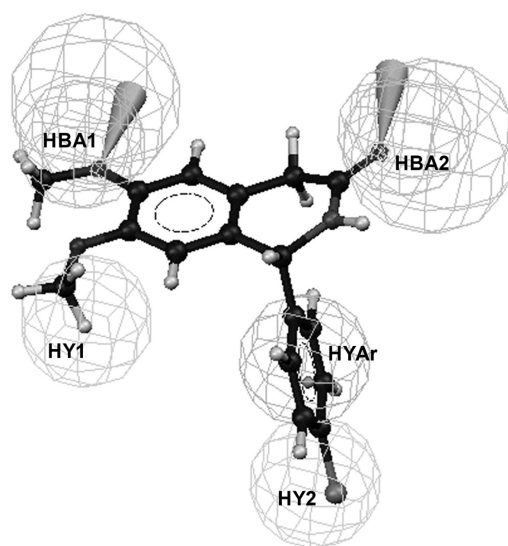
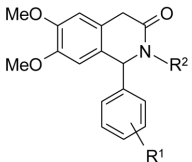


Figure 4. Compound **21c** mapped into HypoGen pharmacophore model Hypo1. The pharmacophore features are labeled as follow: hydrogen bond acceptor (HBA1 and HBA2); hydrophobic aromatic region (HYAr.); hydrophobic group (HY1 and HY2).

Table 3. Anticonvulsant activity against audiogenic seizures in DBA/2 mice.


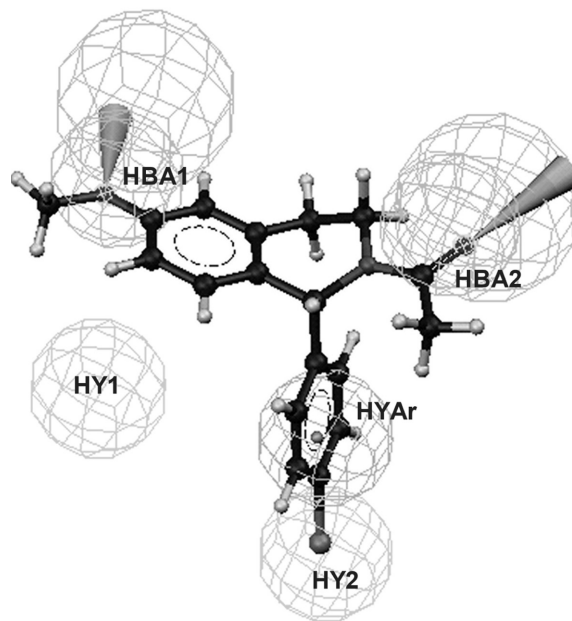
$R^2 = H; 21$
 $R^2 = Ac; 22$

Compd.	R^1	ED_{50} ($\mu\text{mol/kg}$) ^{a)} ($\pm 95\%$ confidence limits)	
		clonic phase	tonic phase
21a	H	> 100	70.1 (60.3–91.0)
21b	4-F	> 100	81.7 (52.5–127)
21c	4-Cl	23.4 (14.4–36.9)	17.6 (12.8–25.6)
21d	4-Br	> 100	> 100
21e	4-NO ₂	96.9 (60.5–155)	58.3 (41.3–82.3)
21f	3-NO ₂	> 100	74.1 (50.6–108)
22a	H	> 100	> 100
22b	4-F	> 100	92.5 (55.1–155)
22c	4-Cl	> 100	63.8 (45.1–90.2)
22d	4-Br	> 100	> 100
22e	4-NO ₂	84.6 (64.5–111)	44.9 (26.6–75.8)
22f	3-NO ₂	> 100	> 100

^{a)} All data were calculated according to the method of Litchfield and Wilcoxon [23]. At least 32 animals were used to calculate each ED_{50} .

Secondly, we extended our investigation and decided to explore if the two methoxy groups were important for anticonvulsant activity as suggested by our predictive pharmacophore model. We have thus studied C-6-monomethoxytetrahydroisoquinolines **23a–f** and **24a–f** (Fig. 3), where the original feature interacting with the hydrophobic region HY1 was lacking, and synthesized them via the route outlined in Scheme 2.

Compound **24c**, which is the analogue of the most active TS compound **4** (experimental $ED_{50} = 4.2 \mu\text{mol/kg}$),

**Figure 5.** Structure of compound **24c** superimposed on model Hypo1. The pharmacophore features are labeled as follow: hydrogen bond acceptor (HBA1 and HBA2); hydrophobic aromatic region (HYAr); hydrophobic group (HY1 and HY2).

should show lower efficacy than the corresponding 6,7-disubstituted derivative **4** (the estimated ED_{50} value for compound **24c** is $77 \mu\text{mol/kg}$), since one chemical feature of model Hypo1 is not mapped (Fig. 5).

As expected, the anticonvulsant pharmacological screening confirms our *in silico* analysis, as **24c** (Table 4) was really less active than analogue **4**. The same behavior was observed for compounds **23a–f** and **24a–f** (Table 4), which showed generally lower anticonvulsant properties with respect to 6,7-dimethoxy analogues [12, 14].

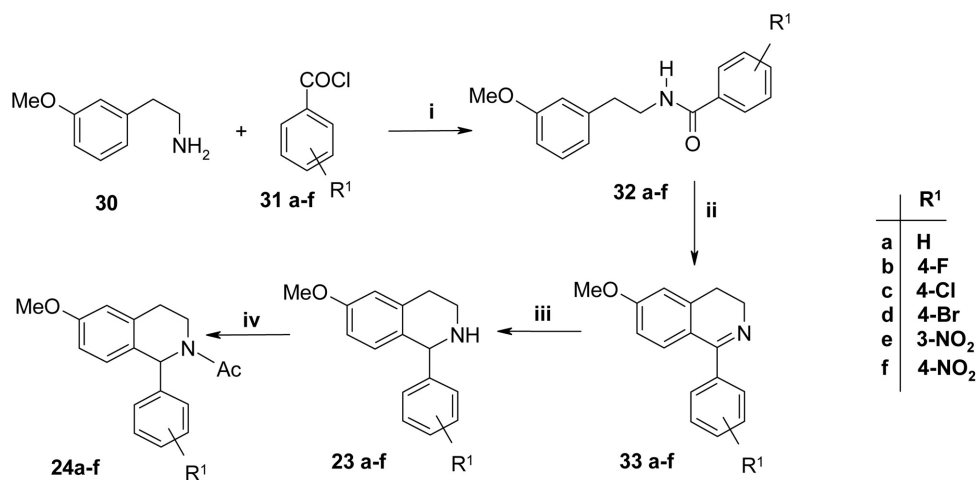
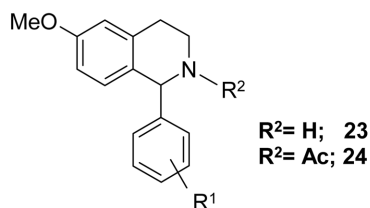
**Scheme 2.** Synthesis of C-6-monomethoxytetrahydroisoquinolines **23a–f** and **24a–f**.

Table 4. Anticonvulsant activity against audiogenic seizures in DBA/2 mice.

Compd.	R ¹	ED ₅₀ (μmol/kg) ^{a)} (±95% confidence limits)	
		clonic phase	tonic phase
23a	H	84.4 (59.4–121)	35.8 (24.2–53.1)
23b	4–F	48.4 (29.7–79.0)	16.0 (9.26–27.5)
23c	4–Cl	>100	>100
23d	4–Br	>100	56.5 (38.0–84.0)
23e	4–NO ₂	32.0 (21.1–48.6)	3.30 (2.11–5.16)
23f	3–NO ₂	82.8 (51.2–134)	32.0 (18.7–56.6)
24a	H	41.5 (28.2–61.1)	3.60 (2.02–6.41)
24b	4–F	>100	>100
24c	4–Cl	82.5 (63.6–107)	53.4 (36.5–78.2)
24d	4–Br	>100	>100
24e	4–NO ₂	64.5 (42.7–97.3)	21.2 (15.1–29.7)
24f	3–NO ₂	65.9 (39.3–110)	23.8 (15.0–37.9)

^{a)} All data were calculated according to the method of Litchfield and Wilcoxon [23]. At least 32 animals were used to calculate each ED₅₀.

Moreover, the HypoGen pharmacophore Hypo1 was also useful to explore the influence of *N*-substitution on biological activity. Thus, we studied the *N*-substituted derivatives **25a–f**, **26a–f**, and **27** (see Fig. 3) having functionalities able to engage hydrogen bond as requested by

our pharmacophore model. In particular Hypo1 suggested that some compounds, such as **25c**, **26c**, and **27**, could be potential anticonvulsant agents with an estimated ED₅₀ values of 24 μmol/kg, 4.3 μmol/kg and 12 μmol/kg, respectively; the superimposition of their structures against the 3D hypothesis revealed that the five features of the pharmacophore were well matched by the chemical groups of the molecules (Fig. 6). So we prepared compounds **25a–f**, **26a–f**, and **27** following the synthetic pathway outlined in Scheme 3.

The results of experimental ED₅₀ values against audiogenic seizures in DBA/2 mice (Table 5) for **25c** (82.79 μmol/kg), **26c** (68.7 μmol/kg), and **27** (57.36 μmol/kg) were not in agreement with the estimated activities. Moreover, this new series of *N*-substituted tetrahydroisoquinolines generally demonstrates poor efficacy against audiogenic seizures.

The discrepancy between predict and actual ED₅₀ values could be explained considering that a long chain around the carbonyl group might occupy a region where the increased steric bulk alters the ability of these compounds to bind to the receptor.

Since our Hypo1 model did not take into account steric factors that might be important for the binding affinity, we subsequently decided to optimize our pharmacophore-based 3D model by including compounds **25c**, **26c**, and **27** in the TS and by using the algorithm Catalyst/HypoRefine [16], which performs automated generation of excluded volumes in activity-based hypothesis generation. In fact, for systems where steric effect plays a role in modulating biological activity, HypoRefine is able to add one or more excluded volumes to HypoGen models in order to improve both the regression coefficients and the

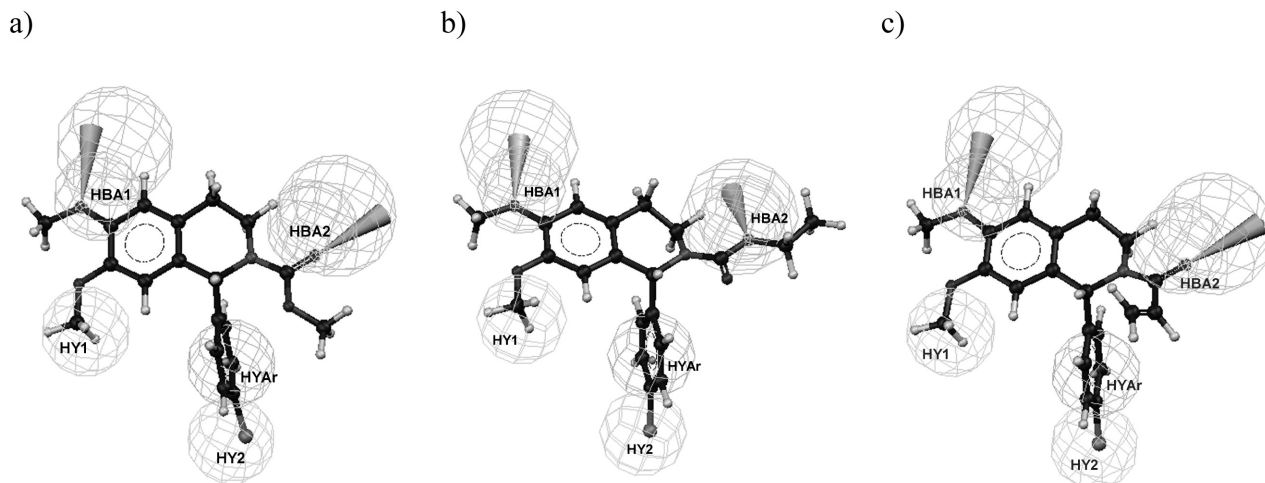
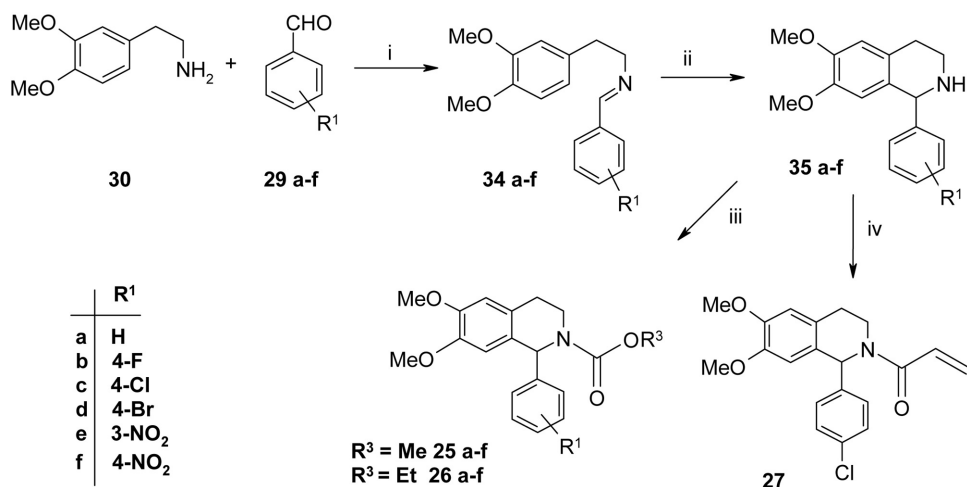


Figure 6. Mapping of compounds **25c** (a), **26c** (b), and **27** (c) onto the best five-feature hypothesis Hypo1. The pharmacophore features are labeled as follow: hydrogen bond acceptor (HBA1 and HBA2); hydrophobic aromatic region (HYAr,); hydrophobic group (HY1 and HY2).



Scheme 3. Synthesis of compounds 25a–f, 26a–f, and 27.

Table 5. Anticonvulsant activity against audiogenic seizures in DBA/2 mice.

Compd.	R ¹	ED ₅₀ (μmol/kg) ^{a)} (± 95% confidence limits)	
		clonic phase	tonic phase
25a	H	> 100	38.9 (24.2–62.4)
25b	4-F	> 100	43.1 (23.9–77.7)
25c	4-Cl	82.8 (51.2–134)	45.5 (27.8–74.3)
25d	4-Br	> 100	> 100
25e	4-NO ₂	61.7 (40.8–93.5)	16.4 (10.7–25.3)
25f	3-NO ₂	53.7 (35.9–80.2)	13.0 (8.26–20.5)
26a	H	> 100	68.7 (40.5–116)
26b	4-F	36.1 (18.7–69.5)	10.8 (5.43–21.6)
26c	4-Cl	68.7 (40.5–116)	21.0 (10.3–43.1)
26d	4-Br	47.2 (32.6–68.2)	13.3 (7.81–22.8)
26e	4-NO ₂	> 100	> 100
26f	3-NO ₂	> 100	> 100
27	–	57.3 (38.4–85.6)	47.9 (35.9–64.0)

^{a)} All data were calculated according to the method of Litchfield and Wilcoxon [23]. At least 32 animals were used to calculate each ED₅₀.

accuracy of activity predictions, thus providing more realistic pharmacophore-based SAR models.

The algorithm HypoRefine thus allowed the development of a new set of ten hypotheses using the data from the expanded TS and the same Catalyst parameters as in the previous hypothesis run. Our automatically devel-

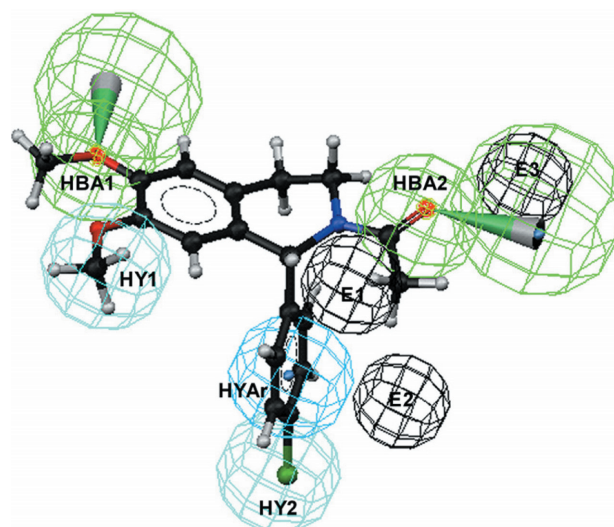


Figure 7. The top-scoring pharmacophore HypoRef1 is mapped to the most active compound in the training set (TS). The pharmacophore features are color-coded as follow: green, hydrogen bond acceptor (HBA1 and HBA2); blue, hydrophobic aromatic region (HYAr); cyan, hydrophobic group (HY1 and HY2); black, excluded volumes (E1, E2, E3).

oped HypoRefine models showed correlation coefficients ranging from 0.619 to 0.945 and a difference between the fixed and null costs of 85.0 bits.

In particular, the most statistically significant hypothesis (Hypo1Ref: correlation coefficient = 0.945; root-mean-square divergence = 1.00; cost difference = 66.380) was chosen as the model for further studies.

Hypo1Ref consisted of the same five chemical features of the previous HypoGen model: two hydrogen-bond acceptors (HBA), one hydrophobic aromatic region (HYAr), and two hydrophobic region (HY); moreover,

Table 6. Actual and estimated ED₅₀ values for the TS molecules based on pharmacophore model Hypo1Ref.

Compd.	Experimental ED ₅₀ (mmol/kg)	Estimated ED ₅₀ (μmol/kg)	Error cost ^{a)}
4	4.2	4.8	+1.2
5	13	14	+1.1
6	19	25	+1.3
7	20	19	-1
8	25	19	-1.3
9	30	25	-1.2
10	32	41	+1.3
11	37	34	-1.1
12	45	93	+2.1
13	49	70	+1.4
14	54	38	-1.4
27	57	43	-1.3
15	63	67	+1.1
26c	69	59	-1.2
16	72	68	-1.1
25c	83	80	-1
17	83	59	-1.4
18	97	95	-1
19	100	120	+1.2
20	130	98	-1.3

^{a)} The error cost values for all TS compounds, expressed as the ratio between the estimated and experimental activities or its negative inverse if the ratio is less than one, were found to be <10 implying a not more than one order difference between estimated and actual activity.

three excluded volumes (E1, E2, E3) were included in the 3D model. As example, the Hypo1Ref hypothesis is shown together with the structure of the most active compound of the TS, **4** (Fig. 7).

Using HypoRef1, the anticonvulsant activities of the twenty TS compounds were predicted correctly within one order of magnitude (Table 6).

In particular, the ED₅₀ values of **25c**, **26c**, and **27** were well estimated with respect to the previous hypothesis Hypo1. In fact, as shown for compound **25c** in Fig. 8, even though these compounds had the five required chemical groups for high potency, the inclusion of the three excluded volume spheres prevented them from matching all pharmacophore features, thus explaining their lower activity.

Chemistry

Synthetic approaches are outlined in Schemes 1-3. Suitable methods were selected to obtain the varied classes of designed isoquinolines starting from different reagents. The 1-aryl-6,7-dimethoxy-1,2-dihydroisoquinolin-3(4*H*)-ones **21a-f** were obtained, according to the literature [17], by condensation of the (3,4-dimethoxyphenyl)acetonitrile **28** with suitable aromatic aldehydes **29a-f** under acid catalysis conditions (Scheme 1). The isoquinolin-

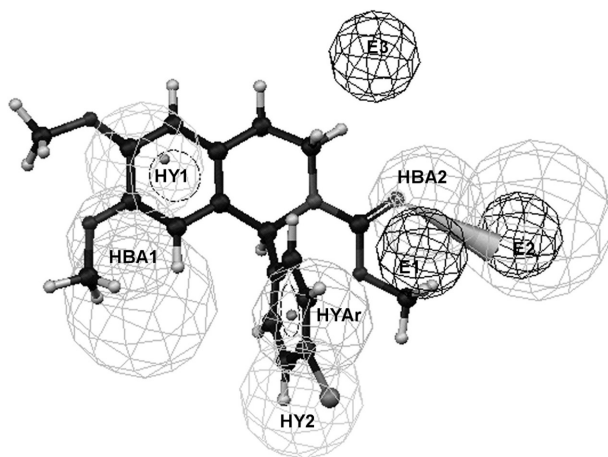


Figure 8. Compound **25c** aligned onto the lowest cost model HypoRef1. The pharmacophore features are labeled as follow: hydrogen bond acceptor (HBA1 and HBA2); hydrophobic aromatic region (HYAr.); hydrophobic group (HY1 and HY2); excluded volumes (E1, E2, E3)

3(2*H*)-one derivatives **21a-f** were further subjected to reaction with acetic anhydride to afford *N*-acetyl derivatives **22a-f** with good yields.

In Scheme 2, the synthetic route for 1-aryl-6-methoxy-1,2,3,4-tetrahydroisoquinolines, **23a-f** and **24a-f**, using the Bischler-Napieralski method [18] is reported. The first step was the synthesis of benzamide derivatives **32a-f** starting from 2-(3'-methoxyphenyl)ethylamine **30** and benzoylchloride derivatives **31a-f** in the presence of Na₂CO₃ solution. By treatment with POCl₃, the benzamide derivatives cyclized giving isoquinolines **33a-f**, which were easily reduced into 1,2,3,4-tetrahydroisoquinolines **23a-f** employing NaBH₄. The corresponding *N*-acetyl derivatives **24a-f** were prepared by reaction with acetic anhydride.

Finally, as shown in Scheme 3, alkyl *N*-carboxylate-1-aryl-6,7-dimethoxy-1,2,3,4-tetrahydroisoquinolines, **25a-f** and **26a-f**, were prepared starting from compounds **35a-f** obtained following the synthetic pathway previously reported by us [14]. The introduction of alkyl *N*-carboxy substituent was realized by reaction with right alkylchloroformates under basic conditions [19]. Attempting to obtain the 3-chloropropionyl substituted derivative, compound **35c** reacted with 3-chloropropionyl chloride affording only the dehydrohalogenated product **27**.

Conclusions

This paper describes the generation of a quantitative pharmacophore model for tetrahydroisoquinoline deriv-

atives acting as anticonvulsant agents. The best HypoGen hypothesis allowed the design of new isoquinoline derivatives (*e.g.* **21c**) able to prevent audiogenic seizures in DBA/2 mice at dose comparable to other known AMPAR noncompetitive antagonists. The synthetic approaches and structural properties have also been reported for all the designed molecules.

Even if none of the new compounds show activity higher than the “lead compound” **4**, this study suggested interesting structure-activity relationships for this class of molecules. In particular, the most important finding was to demonstrate the discrepancy between predict and experimental ED₅₀ values for some *N*-substituted derivatives, by using the excluded volumes approach.

Financial support for this research by MIUR (COFIN2004, Roma, Italy), Fondo di Ateneo per la Ricerca (Università di Messina) and Fondo per gli Investimenti della Ricerca di Base (FIRB 2003) is gratefully acknowledged.

Experimental

Generation of HypoGen-based pharmacophore models

Pharmacophores have been generated with the HypoGen module of Catalyst 4.9 [13] using a TS of 17 1,2,3,4-tetrahydroisoquinoline derivatives.

All molecular structures were sketched within Catalyst and minimized to their closest local energy minimum using a molecular mechanics approach. Poled conformations were generated for each molecule using the “best” conformer generation option and an energy cutoff of 10 kcal/mol.

Five chemical feature types were used in the HypoGen run: hydrogen bond acceptor (HBA), hydrogen bond donor (HBD), hydrophobic (HY), hydrophobic aromatic (HYAr) and positive ionizable (P) groups.

No constraint on the minimum and maximum number of each type of feature in the reported pharmacophore was applied. In the model generation methodology, the interfeature spacing penalty was reduced from its default value to 50 pm. In fact, the default setting of 297 pm is often applicable to large, more flexible molecules, while small, rigid molecules require a lower value. In particular, we reduced the minimum permitted interfeature spacing in order to enable Catalyst to consider features of the TS compounds with a minimum distance of 50 pm as two distinct functions.

The uncertainty value of the compounds activity, which represents the ratio range of uncertainty in the activity value based on the expected statistical variability of biological data collection, was set to 1.3.

All other parameters were kept to their default value.

During the hypothesis generation process, Catalyst selects the best hypothesis from the various possibilities by applying a cost analysis. In fact, HypoGen provides two important theoretical parameters (named “cost values”), that have to be investigated in order to value the simplicity of the models and their statistical significance: the fixed cost (cost of a perfect hypothesis) and the null cost (cost of a hypothesis for which we assume there is no

structure data and the average of all activities in the TS is used as the estimate), both expressed in bits unit. In general, the greater the difference between these cost values, the higher the probability of generating useful models.

The cost value of each optimized pharmacophore should lie somewhere between these two values. Moreover, the difference between the null cost hypothesis and the total hypothesis cost is of particular importance. A true correlation in the data will very likely be estimated by models that exhibit a cost difference (null cost-total cost) of 60 bits or higher. On the other hand, Catalyst documentation suggested that the difference between fixed and null costs should be 70 or higher to achieve this request.

In addition to the cost analysis, two other parameters are involved in establishing the hypothesis significance: RMS (root-mean-square divergence) represents the deviation of the log (estimated activities) from the log (measured activities) normalized by the log (uncertainties) and indicates the quality of “prediction” for the training set, while the correlation (*r*) value is the linear regression derived from the geometric fit index.

In the development of 3D hypothesis by Catalyst Hypofine, the differences in the steric bulk between the most active and the inactive compounds are labeled in the “principal” column of the input spreadsheet; for our study, we chose **4** as the active compound (labeled with digit 2) and the compounds with activities higher than 65 μmol/kg as the inactive ones (labeled with digit 1).

Chemistry

Melting points were determined on a Stuart SMP10 apparatus (Dynalab Corp. Rochester, NY, USA) and are uncorrected. Elemental analyses (C, H, N) were carried out on a Carlo Erba Model 1106 Elemental Analyzer (Carlo Erba, Milan, Italy) and the results are within ±0.4% of the theoretical values. Merck silica gel 60 F₂₅₄ plates were used for analytical TLC; column chromatography was performed on Merck silica gel 60 (70–230 mesh; Merck, Darmstadt, Germany). ¹H-NMR spectra were measured in CDCl₃ or DMSO-d₆ with a Varian Gemini 300 spectrometer (Varian Inc., Palo Alto, CA, USA); chemical shifts are expressed in δ (ppm) relative to TMS as internal standard and coupling constants (*J*) in Hz. All exchangeable protons were confirmed by addition of D₂O.

General procedure for the synthesis of 1-aryl-6,7-dimethoxy-1,2-dihydroisoquinolin-3(4H)-ones, **21a–f**

(3,4-Dimethoxyphenyl)acetonitrile **28** (1 g, 5.6 mmol) was mixed with polyphosphoric acid (3.50 g) at room temperature and heated at 80°C. After addition of the aldehyde derivatives **29a–f** (4.2 mmol) the mixture was heated at 100°C for 2 h and then quenched by adding water. After stirring at room temperature for 1 h, the residue was recovered by filtration and treated with water made basic with ammonium hydroxide. The suspension was heated for 1 h and left overnight at room temperature. The precipitate was filtered off and purified by crystallization with ethyl acetate. By employing the same procedure, compounds **21a** and **21c–f** were previously synthesized [20].

1-(4'-Fluorophenyl)-6,7-dimethoxy-1,2-dihydroisoquinoline-3(4H)-one, **21b**

Mp. 185–187°C. Yield 45%. ¹H-NMR δ: 3.65 (s, 2H, CH₂), 3.71 (s, 3H, MeO-6), 3.89 (s, 3H, MeO-7), 5.58 (s, 1H, H-1), 6.23 (s, 1H, NH), 6.34 (s, 1H, H-5), 6.65 (s, 1H, H-8), 7.03–7.24 (m, 4H, Ar). Anal.

calcd. for $C_{17}H_{16}FNO_3$: C, 67.76; H, 5.53; N, 4.65. Found: C, 67.96; H, 5.43; N, 4.41.

General procedure for the synthesis of 2-acetyl-1-aryl-6,7-dimethoxy-1,2-dihydroisoquinolin-3(4H)-ones, 22a–f

A solution of 1-aryl-6,7-dimethoxy-1,2-dihydroisoquinolin-3(4H)-ones **21a–f** (1 mmol) in acetic anhydride (7–8 mL) was refluxed for 90 min. After cooling, the reaction mixture was quenched by adding H_2O , and the organic layer was extracted with $CHCl_3$, dried over Na_2SO_4 , and then concentrated *in vacuo*. The crude product was crystallized by adding a small amount of diethyl ether. Compounds **22a** was also previously obtained using a similar synthetic procedure [20].

2-Acetyl-1-(4'-fluorophenyl)-6,7-dimethoxy-1,2-dihydroisoquinoline-3(4H)-one, 22b

Mp. 160–164°C. Yield 70%. 1H -NMR δ : 2.65 (s, 3H, MeCO), 3.50 (AB system, 2H, $J = 18.9$, CH_2), 3.90 (s, 3H, MeO-6), 3.91 (s, 3H, MeO-7), 6.73 (s, 1H, H-5), 6.84 (s, 1H, H-8), 6.91 (s, 1H, H-1), 6.95–7.01 (m, 4H, Ar). Anal. calcd. for $C_{19}H_{18}FNO_4$: C, 66.46; H, 5.28; N, 4.08. Found: C, 66.44; H, 5.25; N, 4.12.

2-Acetyl-1-(4'-chlorophenyl)-6,7-dimethoxy-1,2-dihydroisoquinoline-3(4H)-one, 22c

Mp. 166–170°C. Yield 70%. 1H -NMR δ : 2.65 (s, 3H, MeCO), 3.50 (AB system, 2H, $J = 18.9$, CH_2), 3.90 (s, 3H, MeO-6), 3.91 (s, 3H, MeO-7), 6.73 (s, 1H, H-5), 6.82 (s, 1H, H-8), 6.90 (s, 1H, H-1), 6.98 (d, 2H, $J = 8.5$, H2'-H6'), 7.23 (d, 2H, $J = 8.5$, H3'-H5'). Anal. calcd. for $C_{19}H_{18}ClNO_4$: C, 63.42; H, 5.04; N, 3.89. Found: C, 63.22; H, 5.21; N, 3.90.

2-Acetyl-1-(4'-bromophenyl)-6,7-dimethoxy-1,2-dihydroisoquinoline-3(4H)-one, 22d

Mp. 175–177°C. Yield 68%. 1H -NMR δ : 2.65 (s, 3H, MeCO), 3.50 (AB system, 2H, $J = 18.9$, CH_2), 3.90 (s, 3H, MeO-6), 3.91 (s, 3H, MeO-7), 6.73 (s, 1H, H-5), 6.80 (s, 1H, H-8), 6.92 (d, 2H, $J = 8.5$, H2'-H6'), 7.39 (d, 2H, $J = 8.5$, H3'-H5'). Anal. calcd. for $C_{19}H_{18}BrNO_4$: C, 56.45; H, 4.49; N, 3.46. Found: C, 56.41; H, 4.51; N, 3.44.

2-Acetyl-1-(3'-nitrophenyl)-6,7-dimethoxy-1,2-dihydroisoquinoline-3(4H)-one, 22e

Mp. 208–210°C. Yield 55%. 1H -NMR δ : 2.69 (s, 3H, MeCO), 3.53 (AB system, 2H, $J = 18.9$, CH_2), 3.92 (s, 3H, MeO-6), 3.94 (s, 3H, MeO-7), 6.76 (s, 1H, H-5), 6.90 (s, 1H, H-8), 6.94 (s, 1H, H-1), 7.47–8.19 (m, 4H, Ar). Anal. calcd. for $C_{19}H_{18}N_2O_6$: C, 61.62; H, 4.90; N, 7.56. Found: C, 61.60; H, 4.93; N, 7.52.

2-Acetyl-1-(4'-nitrophenyl)-6,7-dimethoxy-1,2-dihydroisoquinoline-3(4H)-one, 22f

Mp. 180–182°C. Yield 45%. 1H -NMR δ : 2.68 (s, 3H, MeCO), 3.50 (AB system, 2H, $J = 18.9$, CH_2), 3.91 (s, 3H, MeO-6), 3.93 (s, 3H, MeO-7), 6.75 (s, 1H, H-5), 6.90 (s, 1H, H-8), 6.94 (s, 1H, H-1), 7.25 (d, 2H, $J = 8.8$, H2'-H6'), 8.14 (d, 2H, $J = 8.8$, H3'-H5k). Anal. calcd. for $C_{19}H_{18}N_2O_6$: C, 61.62; H, 4.90; N, 7.56. Found: C, 61.61; H, 4.85; N, 7.60.

General procedure for the synthesis of 1-aryl-6-methoxy-1,2,3,4-tetrahydroisoquinolines, 23a–f

To a stirred mixture of 2-(3'-methoxyphenyl)ethylamine **30** (1.51 g, 10 mmol) in $CHCl_3$ and 20% aq. K_2CO_3 (10 mL), a solution of the suitable benzoylchloride **31a–f** (11 mmol) in $CHCl_3$ (10 mL) was added drop-wise. The reaction mixture was stirred at room temperature for 3 h and the organic layer was washed consecutively with H_2O , 5% HCl, 20% aq. $NaHCO_3$, H_2O , dried over Na_2SO_4 , and finally the solvent was removed *in vacuo*. The crude product was crystallized by adding a small amount of diethyl ether to give the *N*-[2-(3'-methoxyphenyl)-ethyl]benzamide derivatives **32a–f** as colorless needles. A mixture of the obtained benzamide **32a–f** (5.3 mmol), $POCl_3$ (0.724 mL, 7.7 mmol) and dry toluene was refluxed for 60 min. The solvent and $POCl_3$ were removed under reduced pressure. After addition of 10% NH_4OH , the product was taken up in $AcOEt$ and the organic layer was washed with H_2O , dried over Na_2SO_4 , and then concentrated *in vacuo*. Crystallization of the crude product from diethyl ether gave 1-aryl-3,4-dihydro-6-methoxyisoquinoline **33a–f** as colorless prisms. To a stirred solution of the obtained dihydroisoquinoline **33a–f** (5.5 mmol) in $MeOH$ (20 mL), $NaBH_4$ (0.224 g, 5.9 mmol) was added and the reaction mixture was stirred for 1 h at room temperature. The reaction mixture was quenched by adding H_2O , extracted with $AcOEt$, dried over Na_2SO_4 , and then concentrated at reduced pressure. The crude product was crystallized by adding a small amount of diethyl ether to give 1-aryl-6-methoxy-1,2,3,4-tetrahydroisoquinoline **23b**, **23e–f** as colorless needles. A similar synthetic procedure was previously used for the synthesis of compounds **23a** and **23c–d** [18].

1-(4'-Fluorophenyl)-6-methoxy-1,2,3,4-tetrahydroisoquinoline, 23b

Mp. 94–98°C. Yield 53%. 1H -NMR δ : 2.81–3.22 (m, 2H, CH_2-CH_2), 3.78 (s, 3H, MeO-6), 5.03 (s, 1H, H-1), 6.63 (m, 3H, H-7, H-8, H-5), 6.97–7.23 (m, 4H, Ar). Anal. calcd. for $C_{16}H_{16}FNO$: C, 74.69; H, 6.25; N, 5.44. Found: C, 74.41; H, 6.02; N, 5.79.

1-(3'-Nitrophenyl)-6-methoxy-1,2,3,4-tetrahydroisoquinoline, 23e

Mp. 52–54°C. Yield 61%. 1H -NMR δ : 2.84–3.21 (m, 2H, CH_2-CH_2), 3.80 (s, 3H, MeO-6), 5.17 (s, 1H, H-1), 6.61–6.71 (m, 3H, H-8, H-5, H-7), 7.49 (t, 1H, $J = 7.7$, H-5'), 7.64 (d, 1H, $J = 7.7$, H-6'), 8.13 (s, 1H, H-2'), 8.17 (d, 1H, $J = 8.0$, H-4'). Anal. calcd. for $C_{16}H_{16}N_2O_3$: C, 67.59; H, 5.67; N, 9.85. Found: C, 67.33; H, 5.83; N, 9.62.

1-(4'-Nitrophenyl)-6-methoxy-1,2,3,4-tetrahydroisoquinoline, 23f

Mp. 67–70°C. Yield 60%. 1H -NMR δ : 2.85–3.20 (m, 2H, CH_2-CH_2), 3.79 (s, 3H, MeO-6), 5.16 (s, 1H, H-1), 6.57–6.68 (m, 3H, H-8, H-5, H-7), 7.46 (d, 2H, $J = 8.5$, H2'-H6'), 8.18 (d, 2H, $J = 8.2$, H3'-H5'). Anal. calcd. for $C_{16}H_{16}N_2O_3$: C, 67.59; H, 5.67; N, 9.85. Found: C, 67.23; H, 5.85; N, 9.57.

General procedure for the synthesis of 2-acetyl-1-aryl-6-methoxy-1,2,3,4-tetrahydroisoquinolines, 24a–f

A solution of 1-aryl-6-methoxy-1,2,3,4-tetrahydroisoquinolines **23a–f** (1 mmol) in acetic anhydride (7–8 mL) was refluxed for

90 min and then cooled, the reaction was quenched by adding H₂O. The organic layer, extracted with CHCl₃, was dried over Na₂SO₄ and then concentrated *in vacuo*. The crude product was crystallized by adding a small amount of diethyl ether.

2-Acetyl-6-methoxy-1-phenyl-1,2,3,4-tetrahydroisoquinoline, 24a

Mp. 105–112°C. Yield 60%. ¹H-NMR δ: 2.17 (s, 3H, -COCH₃), 2.77–3.69 (m, 2H, CH₂-CH₂), 3.81 (s, 3H, MeO-6), 6.73 (m, 1H, H-5), 6.75–6.79 (m, 1H, H-8), 6.89 (s, 1H, H-1), 7.00 (s, 1H, H-7), 7.19–7.31 (m, 5H, Ar). Anal. calcd. for C₁₈H₁₉NO₂: C, 76.84; H, 6.81; N, 4.98. Found: C, 76.53; H, 6.97; N, 5.21.

2-Acetyl-1-(4'-fluorophenyl)-6-methoxy-1,2,3,4-tetrahydroisoquinoline, 24b

Mp. 94–98°C. Yield 55%. ¹H-NMR δ: 2.17 (s, 3H, -COCH₃), 2.77–3.79 (m, 2H, CH₂-CH₂), 3.82 (s, 3H, MeO-6), 6.72 (m, 1H, H-5), 6.75–6.79 (m, 1H, H-8), 6.85 (s, 1H, H-1), 6.91–7.21 (m, 5H, Ar & H-7). Anal. calcd. for C₁₈H₁₈FNO₂: C, 72.22; H, 6.06; N, 4.68. Found: C, 71.86; H, 6.41; N, 4.51.

2-Acetyl-1-(4'-chlorophenyl)-6-methoxy-1,2,3,4-tetrahydroisoquinoline, 24c

Mp. 76–79°C. Yield 58%. ¹H-NMR δ: 2.17 (s, 3H, -COCH₃), 2.77–3.78 (m, 2H, CH₂-CH₂), 3.81 (s, 3H, MeO-6), 6.73 (s, 1H, H-5), 6.75–6.79 (m, 1H, H-8), 6.84 (s, 1H, H-1), 6.97 (s, 1H, H-7), 7.15 (d, 2H, J = 8.5, H₂'-H₆'), 7.23 (d, 2H, J = 8.2, H₃'-H₅'). Anal. calcd. for C₁₈H₁₈ClNO: C, 68.46; H, 5.75; N, 4.44. Found: C, 68.32; H, 5.96; N, 4.21.

2-Acetyl-1-(4'-bromophenyl)-6-methoxy-1,2,3,4-tetrahydroisoquinoline, 24d

Mp. 85–88°C. Yield 62%. ¹H-NMR δ: 2.17 (s, 3H, -COCH₃), 2.76–3.72 (m, 2H, CH₂-CH₂), 3.81 (s, 3H, MeO-6), 6.72 (m, 1H, H-5), 6.75–6.79 (m, 1H, H-8), 6.82 (s, 1H, H-1), 6.97 (s, 1H, H-7), 7.09 (d, 2H, J = 8.5, H₂'-H₆'), 7.38 (d, 2H, J = 8.2, H₃'-H₅'). Anal. calcd. for C₁₈H₁₈BrNO₂: C, 60.10; H, 5.04; N, 3.89. Found: C, 59.89; H, 5.27; N, 3.78.

2-Acetyl-1-(3'-nitrophenyl)-6-methoxy-1,2,3,4-tetrahydroisoquinoline, 24e

Mp. 62–63°C. Yield 60%. ¹H-NMR: 2.20 (s, 3H, -COCH₃), 2.80–3.78 (m, 2H, CH₂-CH₂), 3.83 (s, 3H, MeO-6), 6.75 (m, 1H, H-5), 6.76–6.82 (m, 1H, H-8), 6.90 (s, 1H, H-1), 7.00 (s, 1H, H-7), 7.46 (t, 1H, J = 8.0, H-5'), 7.70 (s, 1H, H-6'), 7.96 (s, 1H, H-2'), 8.09 (d, 1H, J = 8.0, H-4'). Anal. calcd. for C₁₈H₁₈N₂O₄: C, 66.25; H, 5.56; N, 8.58. Found: C, 66.13; H, 5.82; N, 8.79.

2-Acetyl-1-(4'-nitrophenyl)-6-methoxy-1,2,3,4-tetrahydroisoquinoline, 24f

Mp. 65–68°C. Yield 65%. ¹H-NMR d: 2.20 (s, 3H, -COCH₃), 2.80–3.78 (m, 2H, CH₂-CH₂), 3.83 (s, 3H, MeO-6), 6.75 (m, 1H, H-5), 6.76–6.82 (m, 1H, H-8), 6.90 (s, 1H, H-1), 7.00 (s, 1H, H-7), 7.46 (d, 2H, J = 8.5, H₂'-H₆'), 8.18 (d, 2H, J = 8.2, H₃'-H₅'). Anal. calcd. for C₁₈H₁₈N₂O₄: C, 66.25; H, 5.56; N, 8.58. Found: C, 66.02; H, 5.34; N, 8.47.

General procedure for the synthesis of alkyl-1-aryl-6,7-dimethoxy-1,2,3,4-tetrahydroisoquinoline-2-carboxylate, 25a–f and 26a–f

To a solution of 1-aryl-6,7-dimethoxy-1,2,3,4-tetrahydroisoquinoline derivative **35a–f** (2 mmol) in CHCl₃ were added triethylamine (0.28 mL, 2 mmol) and the suitable alkyl chloroformate (2 mmol). The reaction mixture was stirred at room temperature for 90 min and then concentrated *in vacuo*. The crude product was crystallized by adding a small amount of diethyl ether. Compound **25a** was previously obtained by other authors but using a different synthetic approach [21]. Compounds **26a–d** and **26f** were obtained according to the literature method [19].

Methyl-1-(4'-fluorophenyl)-6,7-dimethoxy-1,2,3,4-tetrahydroisoquinoline-2-carboxylate, 25b

Mp. 69–73°C. Yield 48%. ¹H-NMR δ: 2.62–3.83 (m, 4H, CH₂-CH₂), 3.62 (s, 3H, MeO-6), 3.65 (s, 3H, COOMe), 3.73 (s, 3H, MeO-7), 6.20 (s, 1H, H-5), 6.69 (s, 1H, H-8), 6.79 (s, 1H, H-1), 7.09–7.20 (m, 4H, Ar). Anal. calcd. for C₁₉H₂₀FNO₄: C, 67.08; H, 5.84; N, 4.06. Found: C, 66.82; H, 5.51; N, 4.29.

Methyl-1-(4'-chlorophenyl)-6,7-dimethoxy-1,2,3,4-tetrahydroisoquinoline-2-carboxylate, 25c

Mp. 101–104°C. Yield 65%. ¹H-NMR d: 2.68–3.81 (m, 4H, CH₂-CH₂), 3.63 (s, 3H, MeO-6), 3.65 (s, 3H, COOMe), 3.73 (s, 3H, MeO-7), 6.19 (s, 1H, H-5), 6.72 (s, 1H, H-8), 6.80 (s, 1H, H-1), 7.16 (d, 2H, J = 8.2, H₂'-H₆'), 7.37 (d, 2H, J = 8.2, H₃'-H₅'). Anal. calcd. for C₁₉H₂₀ClNO₄: C, 63.07; H, 5.57; N, 3.87. Found: C, 63.32; H, 5.28; N, 3.55.

Methyl-1-(4'-bromophenyl)-6,7-dimethoxy-1,2,3,4-tetrahydroisoquinoline-2-carboxylate, 25d

Mp. 109–111°C. Yield 58%. ¹H-NMR δ: 2.67–3.82 (m, 4H, CH₂-CH₂), 3.63 (s, 3H, MeO-6), 3.65 (s, 3H, COOMe), 3.73 (s, 3H, MeO-7), 6.17 (s, 1H, H-5), 6.72 (s, 1H, H-8), 6.79 (s, 1H, H-1), 7.10 (d, 2H, J = 8.5, H₂'-H₆'), 7.50 (d, 2H, J = 8.5, H₃'-H₅'). Anal. calcd. for C₁₉H₂₀BrNO₄: C, 56.17; H, 4.96; N, 3.45. Found: C, 56.48; H, 4.41; N, 3.72.

Methyl-1-(3'-nitrophenyl)-6,7-dimethoxy-1,2,3,4-tetrahydroisoquinoline-2-carboxylate, 25e

Mp. 155–157°C. Yield 58%. ¹H-NMR d: 2.66–3.84 (m, 4H, CH₂-CH₂), 3.63 (s, 3H, MeO-6), 3.67 (s, 3H, COOMe), 3.75 (s, 3H, MeO-7), 6.33 (s, 1H, H-5), 6.83 (s, 2H, H-8, H-1), 7.59–7.63 (m, 2H, H-5', H-6'), 7.97 (s, 1H, H-2'), 8.13 (d, 1H, J = 5.50, H-4'). Anal. calcd. for C₁₉H₂₀N₂O₆: C, 61.28; H, 5.41; N, 7.52. Found: C, 61.05; H, 5.12; N, 7.83.

Methyl-1-(4'-nitrophenyl)-6,7-dimethoxy-1,2,3,4-tetrahydroisoquinoline-2-carboxylate, 25f

Mp. 157–160°C. Yield 48%. ¹H-NMR δ: 2.65–3.84 (m, 4H, CH₂-CH₂), 3.65 (s, 3H, MeO-6), 3.66 (s, 3H, COOMe), 3.74 (s, 3H, MeO-7), 6.29 (s, 1H, H-5), 6.82 (s, 2H, H-8, H-1), 7.46 (d, 2H, J = 8.5, H₂'-H₆'), 8.17 (d, 2H, J = 8.5, H₃'-H₅'). Anal. calcd. for C₁₉H₂₀N₂O₆: C, 61.28; H, 5.41; N, 7.52. Found: C, 61.12; H, 5.22; N, 7.31.

Ethyl-1-(3'-nitrophenyl)-6,7-dimethoxy-1,2,3,4-tetrahydroisoquinoline-2-carboxylate, 26e

Mp. 66–70°C. Yield 59%. ¹H-NMR δ: 1.21 (t, 3H, J = 6.9, -CH₂CH₃), 2.72–3.85 (m, 4H, CH₂-CH₂), 3.62 (s, 3H, MeO-6), 3.75 (s, 3H, MeO-7), 4.10 (q, 2H, J = 6.9, -CH₂CH₃), 6.32 (s, 1H, H-5), 6.83 (s, 2H, H-8, H-1), 7.61–7.62 (m, 2H, H-5', H-6'), 8.00 (s, 1H, H-2'), 8.11–8.15 (m, 1H, H-4'). Anal. calcd. for C₂₀H₂₂N₂O₆: C, 62.17; H, 5.74; N, 7.25. Found: C, 62.25; H, 5.43; N, 7.32.

Synthesis of 1-(1-(4'-chlorophenyl)-6,7-dimethoxy-1,2,3,4-tetrahydroisoquinolinyl)prop-2-en-1-one, 27

To a solution of 1-(4'-chlorophenyl)-6,7-dimethoxy-1,2,3,4-tetrahydroisoquinoline 35c (0.8 g, 2.64 mmol) in CHCl₃ were added triethylamine (1.1 mL, 2.64 mmol) and 3-chloropropionyl chloride (0.25 mL, 2.64 mmol). The reaction mixture was stirred at room temperature for 90 min and then concentrated *in vacuo*. The crude product was crystallized by adding a small amount of diethyl ether. Mp. 100–102°C. Yield 50%. ¹H-NMR δ: 2.38–3.50 (m, 4H, CH₂-CH₂), 3.77 (s, 3H, MeO-6), 3.89 (s, 3H, MeO-7), 5.75 (m, 1H, CH=CH_{2a}), 6.45 (m, 1H, CH=CH_{2b}), 6.51 (s, 1H, H-5), 6.61 (m, 1H, CH=CH₂), 6.66 (s, 1H, H-8), 6.89 (s, 1H, H-1), 7.19–7.24 (m, 4H, Ar). Anal. calcd. for C₂₀H₂₀ClNO₃: C, 67.13; H, 5.63; N, 3.91. Found: C, 67.25; H, 5.41; N, 3.80.

Pharmacology

Testing of anticonvulsant activity

All experiments were performed with DBA/2 mice which are genetically susceptible to sound-induced seizures. DBA/2 mice (8–12 g; 22–25 days-old) were purchased from Harlan Italy (Correzzano, Italy). Groups of ten mice of either sex were exposed to auditory stimulation 30 min following administration of vehicle or each dose of drugs studied [22]. The compounds were given intraperitoneally (*ip.*) (0.1 mL/10 g of body weight of the mouse) as a freshly-prepared solution in 50% dimethylsulfoxide (DMSO) and 50% sterile saline (0.9% NaCl). Individual mice were placed under a hemispheric perspex dome (diameter 58 cm), and 60 s were allowed for habituation and assessment of locomotor activity. Auditory stimulation (12–16 kHz, 109 dB) was applied for 60 s or until tonic extension occurred, and induced a sequential seizure response in control DBA/2 mice, consisting of an early wild running phase, followed by generalized myoclonus and tonic flexion and extension sometimes followed by respiratory arrest. The control and drug-treated mice were scored for latency to and incidence of the different phases of the seizures.

The experimental protocol and all the procedures involving animals and their care were conducted in conformity with the institutional guidelines and the European Council Directive of laws and policies.

Statistical analysis

Statistical comparisons between groups of control and drug-treated animals were made using Fisher's exact probability test (incidence of the seizure phases). The ED₅₀ values of each phase of audiogenic seizures was determined for each dose of com-

pound administered, and dose-response curves were fitted using a computer program by Litchfield and Wilcoxon's method [23].

References

- [1] R. Dingleline, K. Borges, D. Bowie, S. F. Traynelis, *Pharmacol. Rev.* **1999**, 51, 7–61.
- [2] R. Gitto, M. L. Barreca, L. De Luca, A. Chimirri, *Expert Opin. Ther. Patents* **2005**, 14, 1199–1213.
- [3] G. De Sarro, R. Gitto, E. Russo, G. F. Ibbadu, *et al.*, *Curr. Top. Med. Chem.* **2005**, 5, 31–42.
- [4] A. Chimirri, G. De Sarro, A. De Sarro, R. Gitto, *et al.*, *J. Med. Chem.* **1997**, 40, 1258–1269.
- [5] R. Gitto, V. Orlando, S. Quartarone, G. De Sarro, *et al.*, *J. Med. Chem.* **2003**, 46, 3758–3761.
- [6] F. András, *Drugs Future* **2001**, 26, 754–756.
- [7] N. Armstrong, E. Gouaux, *Neuron* **2000**, 28, 165–181.
- [8] Y. P. Auberson, *Drugs Future* **2001**, 26, 463–471.
- [9] L. De Luca, A. Macchiarulo, G. Costantino, M. L. Barreca, *et al.*, *Farmaco* **2003**, 58, 107–113.
- [10] A. Chimirri, G. De Sarro, S. Quartarone, M. L. Barreca, *et al.*, *Pure Appl. Chem.* **2004**, 76, 931–939.
- [11] M. L. Barreca, R. Gitto, S. Quartarone, L. De Luca, *et al.*, *J. Chem. Inf. Comput. Sci.* **2003**, 43, 651–655.
- [12] R. Gitto, M. L. Barreca, L. De Luca, G. De Sarro, *et al.*, *J. Med. Chem.* **2003**, 46, 197–200.
- [13] Catalyst, 4.9, Accelrys Inc., San Diego, CA, USA.
- [14] R. Gitto, R. Caruso, V. Orlando, S. Quartarone, *et al.*, *Farmaco* **2004**, 59, 7–12.
- [15] M. L. Barreca, R. Caruso, L. De Luca, R. Gitto, *et al.*, 14th Camerin–Noordwijkerouth Symposium: *Ongoing progress in the receptor chemistry Proceedings* **2003**, 84.
- [16] <http://www.accelrys.com/catalyst/hyporefine.html>.
- [17] G. Deak, K. Gall–Istok, L. Sterk, *Acta Chim. Acad. Sci. Hung.* **1976**, 88, 87–92.
- [18] S. Doi, N. Shirai, Y. Sato, *J. Chem. Soc., Perkin Trans I* **1997**, 15, 2217–2221.
- [19] A. Venkov, N. Mollov, *Dokl. Bulg. Akad. Nauk.* **1979**, 32, 895–897.
- [20] V. St Georgiev, R. G. Van Inwegen, P. Carlson, *Eur. J. Med. Chem.* **1990**, 25, 375–378.
- [21] G. K. Cheung, M. J. Earle, R. A. Fairhurst, H. Heaney, *et al.*, *Synlett* **1991**, 10, 721–723.
- [22] A. G. Chapman, M. J. Croucher, B. S. Meldrum, *Arzneimittelforschung* **1984**, 34, 1261–1264.
- [23] J. T. Litchfield, F. Wilcoxon, *J. Pharmacol. Exp. Ther.* **1949**, 96, 99–113.